Published in final edited form as:
FEBS J. 2013 August ; 280(15): 3621–3631. doi:10.1111/febs.12352.

Differences In Oxygen-Dependent Nitric Oxide Metabolism By Cytoglobin And Myoglobin Account For Their Differing Functional Roles

Xiaoping Liu[*], **Jianjing Tong**, **Joseph R. Zweier**, **Douglas Follmer**, **Craig Hemann**, **Raed Ismail**, and **Jay L. Zweier**[*]

Davis Heart and Lung Research Institute and Department of Internal Medicine, The Ohio State University College of Medicine, 473 West 12th Avenue, Columbus, Ohio 43210

Abstract

The endogenous vasodilator nitric oxide (NO) is metabolized in tissues in an O_2-dependent manner. In skeletal and cardiac muscle, high concentrations of myoglobin (Mb) function as a potent NO scavenger. However, Mb concentration is very low in vascular smooth muscle where low concentrations of cytoglobin (Cygb) may play a major role in metabolizing NO. Questions remain regarding how low concentrations of Cygb and Mb differ in their NO metabolism and the basis for their different cellular roles and functions. In this study, electrode techniques were applied to perform comparative measurements of the kinetics of NO consumption by Mb and Cygb. UV/Vis spectroscopic methods and computer simulations were performed to study the reaction of Mb and Cygb with ascorbate (Asc) and the underlying mechanism. It was observed that the initial rate of $Cygb^{3+}$ reduction by Asc was 415-fold greater than that of Mb^{3+}. In the low [O_2] range (0-50 μM), Cygb-mediated NO consumption rate is ~500 times more sensitive to changes in O_2 concentration than that of Mb. The reduction of $Cygb^{3+}$ by Asc follows a reversible kinetic model while its reduction of Mb^{3+} is irreversible. A reaction mechanism for $Cygb^{3+}$ reduction by Asc was proposed and the reaction equilibrium constants determined. Our results suggest that the rapid reduction of Cygb by cellular reductants enables Cygb to efficiently regulate NO metabolism in the vascular wall in an oxygen-dependent manner, while the slow rate of Mb reduction does not provide this oxygen dependence.

Keywords

Cytoglobin; myoglobin; ascorbate; nitric oxide; oxygen; metabolism kinetics

Introduction

Recent evidence has shown that cytoglobin (Cygb) is expressed not only in adventitial fibroblasts but also in smooth muscle cells [1, 2], playing a role in vascular nitric oxide (NO) catabolism. NO is an important signaling molecule regulating vascular tone or

[*]Corresponding authors: Xiaoping Liu, PhD 473 West 12th Avenue Columbus, OH 43210, USA Phone: +1 614-292-1305, Fax: +1 614-292-8778 Xiaoping.liu@osumc.edu and Jay L. Zweier, MD 473 West 12th Avenue Columbus, OH 43210, USA Phone: +1 614-247-7788, Fax: +1 614-247-7845 jay.zweier@osumc.edu.

resistance and controlling blood flow[3, 4]. The rate of NO metabolism in the intervascular tissue [5] and in the vascular wall [6] is sensitive to change in O_2 concentration. Cygb metabolizes NO in an O_2-dependent manner [1, 7, 8]. We have recently characterized the kinetics of the O_2-dependent NO metabolism by Cygb in the presence of cellular reductants and demonstrated that Cygb can sensitively transduce a change in O_2 concentration to a change in the rate of NO consumption [9], allowing Cygb to sense and regulate the NO diffusion distance in the vascular wall in response to changes in O_2 concentration. However, metabolism of NO is not unique to Cygb. Other globins such as hemoglobin (Hb), myoglobin (Mb) and neuroglobin (Ngb) also metabolize NO [7, 8, 10, 11], and the reaction rates of NO with oxyhemoglobin ($Hb^{2+}O_2$), oxymyoglobin ($Mb^{2+}O_2$), oxyneuroglobin ($Ngb^{2+}O_2$), and oxycytoglobin ($Cygb^{2+}O_2$) are very rapid and similar to each other.

Each of the globins has a unique pattern of cellular expression and localization. Hb is mainly located in red blood cells [12]; Mb is mainly located in heart and skeletal muscles [13]; and Ngb is mainly present in neurons [14, 15]. Cygb has been found in fibroblasts and in the vascular wall [1, 2, 16]. The concentration of Hb hemes in blood is ~8 mM and the concentration of Mb in heart and skeletal muscles is several hundred μM or higher. At such high globin concentrations, the rates of NO consumption in blood, heart and skeletal muscles are very rapid so that most NO molecules will be scavenged by Hb or Mb in these locations [17-21]. Unlike Hb and Mb, Cygb concentration in vivo is in the low μM range [22, 23]. At this low concentration, Cygb does not effectively scavenge NO in the vascular wall, but likely plays a role in the regulation of vascular NO concentration. Interestingly Cygb has been reported to have a binding site for ascorbate that may facilitate its role as an effective reducing substrate [8]. Cygb is considered to have a common evolutionary ancestor with Mb [24]. Mb concentrations in the vascular wall are very low if present at all [25]. Thus, the preferential expression of Cygb over Mb in the smooth muscle suggests that there is an important functional benefit or role provided by Cygb but not Mb.

Questions remain regarding whether Cygb and Mb have similar behavior in their reaction rate and kinetics of NO metabolism and regarding the basis for the different roles and functions of these two similar globins. In order to address these questions, in this study we compare Cygb and Mb with regard to their ability to regulate the O_2-dependent NO consumption rate and with regard to the rate of their reduction by the cellular reductant ascorbate. The reaction mechanism of Cygb reduction by ascorbate is also studied and characterized.

Results

Effect of oxygen concentration on the rate of NO consumption by Mb compared to Cygb

It was previously demonstrated that the rate of NO consumption by Cygb ($V_{Cygb\text{-}NO}$) significantly decreases when oxygen concentrations change from 200 μM to 0 μM [9]. In this study, we measured the rate of NO consumption by 0.3 μM Mb in the presence of 300 μM Asc and 400 units/mL SOD with varying oxygen concentration (Fig. 1A). It can be seen that the rate of NO consumption by Mb ($V_{Mb\text{-}NO}$) only slightly decreases as the O_2 concentration decreases. In contrast, NO consumption by 0.3 μM Cygb, 300 μM Asc, and 400 units/mL SOD is much faster under room air and the rate of NO consumption

significantly decreased when O_2 concentration changes from 200 μM (room air) to near 0 μM (anaerobic conditions) (Fig. 1B).

Reduction of Mb^{3+} by ascorbate

A typical change in the UV-Vis spectrum of the reduction of Mb^{3+} by Asc (10 mM) under anaerobic conditions is shown in Fig. 2A. The Soret band of Mb^{3+} (409 nm) shifts to that of the deoxy Mb^{2+} (434 nm) gradually with time, indicating an Asc-dependent reduction of Mb^{3+} to the Mb^{2+}. The reduction rate of Mb^{3+} by Asc was reported as second order, that is, first order with respect to both Mb and Asc concentration [26]. Since Asc concentrations in the experiments were much greater than the Mb concentration, the reduction of Mb^{3+} by Asc in our experiments was a pseudo first order reaction. Using the time course of the change in absorbance at 409 nm, we determined the pseudo first order rate constant (k'_{Mb}) of Mb^{3+} reduction at 4 different Asc concentrations (10, 30, 50 and 100 mM). The experiments at each concentration were performed 5 times (n=5). The second order rate constant of Mb reduction by Asc was then obtained by plotting k'_{Mb} versus Asc concentration as shown in Fig. 2B. The second order rate constant of Mb reduction by Asc was determined as $k_{Mb}=(8.7 \pm 0.3)\times 10^{-2}\ M^{-1}s^{-1}$ (n=5).

Computer simulations of NO consumption by Mb compared to Cygb

Using the rate constants reported in the literature and measured in our experiments (Table 1), we performed computer simulations of $V_{Mb\text{-}NO}$ and $V_{Cygb\text{-}NO}$ at varying O_2 concentration (using Eq. (7) for Mb and using the Equations in our previous paper [9] for Cygb). Experimental parameters in the equations, such as Mb or Cygb concentration [E], Asc concentration [A], oxygen concentration [O_2], and NO concentration [NO], were the same as the values used in the experiments. Since some rate constants and equilibrium constants in Eq. (7) at 37 °C were not available in the literature, the values of these parameters at 37 °C had to be estimated from available data at other temperatures. The reported k_1 for Mb is from $3.1 \times 10^7\ M^{-1}s^{-1}$ to $3.7 \times 10^7\ M^{-1}s^{-1}$ in the temperature range 10 °C to 25 °C [10, 27, 28]. From this temperature dependence of k_1 on Mb, we used $k_1=4.5 \times 10^7\ M^{-1}s^{-1}$ for Mb at 37 °C. The rate constant k_2 for Mb is measured in our experiments as k_{Mb}. The reported k_4 for Mb at 20 °C is $1.7 \times 10^7\ M^{-1}s^{-1}$ and k_{-4} at 20 °C is $1.2 \times 10^{-4}\ s^{-1}$, so the value of k_{-4}/k_4 at 20 °C is 7.1 pM. Considering that when the temperature changes from 20 °C to 37 °C, k_{-3}/k_3 of Mb increases by nearly 5 times [29], we estimated that k_{-4}/k_4 of Mb at 37 °C is 35 pM assuming that k_{-4}/k_4 and k_{-3}/k_3 have a similar temperature dependence. Simulated curves (solid lines) of $V_{Cygb\text{-}NO}$ and $V_{Mb\text{-}NO}$ versus [O_2] are shown in Fig. 3. The simulated curves are a good fit with the experimental $V_{Cygb\text{-}NO}$ (▽) and $V_{Mb\text{-}NO}$ (•) versus [O_2]. From the slopes of NO decay curves immediately after each NO concentration peak (Fig. 1), we can obtain an NO decay rate that is the sum of NO consumption (V_{total}) by Cygb or Mb, by O_2 and physical diffusion out of the solution. The experimental data of $V_{Mb\text{-}NO}$ and $V_{Cygb\text{-}NO}$ in Fig. 3 were obtained by subtracting the rate of NO diffusion out of the solution from V_{total} for Mb and Cygb, repectively [9]. Final parameters used in the simulated curve are listed (bold fonts) in Table 1. Our simulations show that the slope of the $V_{Mb\text{-}NO}$-[O_2] plot (Fig. 3) is mainly contributed by the NO autoxidation rate V_{au} rather than the Mb-mediated NO consumption rate V_{NO}. In contrast, $V_{Cygb\text{-}NO}$ is mainly contributed by the Cygb-mediated NO consumption rate V_{NO} rather than the NO autoxidation rate V_{au}.

The rate equations for Mb and Cygb in this study and our previous paper [9] were derived under steady-state conditions at any given NO concentration. The in vivo NO concentration at a location and at a certain time period can be considered as a steady-state concentration achieved by continuous NO generation and NO consumption. The NO concentration used in this study is 500 nM. Although NO concentrations used in tests of vascular activity can be as high as μM, the physiological NO concentration in the vascular wall for dilating blood vessels may be much lower, which is in the range of nM or below [30]. Very recently, by using ultrasensitive detector cells, it was observed that the average NO concentrations in the cerebellum and the hippocampus are 200 pM or below [31]. Direct experimental measurements of Cygb-mediated NO metabolism at the nM and sub-nM NO concentration range in our experiments are not possible because of the detection limit of NO electrodes. To examine how O_2 regulates $V_{Cygb\text{-}NO}$ under physiological conditions ([NO] in nM to sub-nM range [30] and [Asc] in mM range [32]), we performed computer simulations based on rate equations (7) and (8) in this paper and rate equations in our previous paper [9] to observe changes of $V_{Cygb\text{-}NO}$ and $V_{Mb\text{-}NO}$ versus O_2 concentration at 3 different NO concentrations 10 nM, 1 nM and 0.1 nM (Fig. 4). In these simulations, we defined $V_{Cygb\text{-}NO}$ and $V_{Mb\text{-}NO}$ at PO_2=100 torr (or $[O_2]$=133 μM at 37 °C in buffer solution) as $(V_{100})_{Cygb}$ and $(V_{100})_{Mb}$, respectively (Note: In experiments in air (21% O2) at 37 °C, PO_2 is ~150 mmHg after correcting for saturated vapor pressure, and the O_2 concentration in buffer solution is ~200 μM. The conversion factor from PO_2 (torr) to O_2 concentration (μM) is 200 μM /150 torr=1.33 μM/torr. When PO_2 is 100 torr or 10 torr, the corresponding O_2 concentration in buffer solution at 37 °C is 133 μM or 13 μM, respectively). The maximal PO_2 in arteries under normoxic conditions is near 100 torr [33, 34], so we consider $(V_{100})_{Cygb}$ and $(V_{100})_{Mb}$ to be the maximal rate of NO metabolism that can be achieved at a given NO concentration and other conditions (Table 1) if the reaction occurs in vivo under normoxic conditions. Both $(V_{100})_{Cygb}$ and $(V_{100})_{Mb}$ are dependent on NO concentration. To compare the O_2 dependence of $V_{Cygb\text{-}NO}$ and $V_{Mb\text{-}NO}$ at different NO concentrations, we normalized the rate of NO metabolism $V_{Cygb\text{-}NO}$ and $V_{Mb\text{-}NO}$ (dividing $V_{Cygb\text{-}NO}$ and $V_{Mb\text{-}NO}$ by $(V_{100})_{Cygb}$ and $(V_{100})_{Mb}$, respectively). The normalized rate of NO metabolism increases as $[O_2]$ increases. The O_2 concentration range corresponding to the normalized rate of NO metabolism below 0.9 is the major working range for O_2 concentration to regulate the rate of NO metabolism. From the simulated curves in Fig. 4 we can see that this working range of $[O_2]$ for regulating the Cygb-mediated NO metabolism is from 0 to 41 μM (31 torr at 37 °C). In contrast, the $[O_2]$ working range for regulating the Mb-mediated NO metabolism is only from 0 to 0.43 μM (0.32 torr), nearly 100 times lower than that for Cygb-mediated NO metabolism.

Effect of oxygen concentration on different globin species

The concentrations of each globin species in the reaction system (including 0.5 μM NO, 300 μM Asc, 400 units/mL SOD, 0.3 μM Mb or Cygb and varied $[O_2]$ were calculated from Eqs. (9)-(12) or from equations in our previous study [9], respectively. The simulated concentration changes of $Cygb^{3+}$, $Cygb^{2+}NO$, $Cygb^{2+}O_2$, Mb^{3+}, $Mb^{2+}NO$, and $Mb^{2+}O_2$ versus $[O_2]$ are shown in Fig. 5. The concentrations of $Cygb^{3+}$, $Cygb^{2+}NO$ and $Cygb^{2+}O_2$ were observed to significantly change with $[O_2]$ while the concentrations of Mb^{3+}, $Mb^{2+}NO$ and $Mb^{2+}O_2$ change very little when $[O_2]$ is lowered from 200 μM down to ~0.2 μM (Figs. 5A & 5B). When $[O_2]$ varies from 0 to 50 μM, $Mb^{2+}O_2$ concentration only increases from 0

to 0.35 pM, while in contrast the $Cygb^{2+}O_2$ concentration increases much more from 0 to 0.17 nM (Fig. 5B). Therefore, the concentration increase of $Cygb^{2+}O_2$ is nearly 500 times greater than the concentration increase of $Mb^{2+}O_2$ in the low oxygen concentration range between 0 and 50 μM.

Kinetic measurements of $Cygb^{3+}$ and Mb^{3+} reduction by ascorbate at different concentrations

Since $Cygb^{3+}$ reduction by Asc is much faster than Mb^{3+}, we further examined if the mechanism for $Cygb^{3+}$ reduction is different from that for Mb^{3+} reduction. It was observed that the reduction of Mb^{3+} to Mb^{2+} by either 10 mM or 30 mM Asc went to completion, albeit rather slowly (Fig. 6A). In contrast, Asc can only partially reduce $Cygb^{3+}$ to $Cygb^{2+}$, with the final ratio of $Cygb^{2+}$ concentration to the initial $Cygb^{3+}$ concentration increasing with Asc concentration, reaching an equilibrium between the reactants and products at each given Asc concentration, To simultaneously record $Cygb^{3+}$ reduction (absorbance peak at 416 nm) and $Cygb^{2+}$ formation (absorbance peak at 428 nm), the reduction process of $Cygb^{3+}$ was recorded by repetitively scanning from 350 nm to 700 nm on a Cary 50 UV/VIS spectrophotometer while different concentrations of Asc (0.1, 0.2, 0.7, 2, 7, 20 mM) were injected into the chamber. From these recorded spectra, we can examine the kinetic characteristics of conversion of $Cygb^{3+}$ to $Cygb^{2+}$ by plotting the absorbance changes vs. time at wavelengths 416 nm and 428 nm (Fig. 6B).

Reaction mechanism of $Cygb^{3+}$ reduction by Asc

The large difference between reduction of Mb^{3+} and $Cygb^{3+}$ by Asc prompts us to think if the reaction kinetics and mechanism for $Cygb^{3+}$ reduction by Asc has some difference from Mb^{3+} reduction by Asc. The formation of different equilibrium concentrations between $Cygb^{2+}$ and $Cygb^{3+}$ at different concentrations of Asc suggests that the reduction of $Cygb^{3+}$ by Asc is a reversible reaction. Furthermore, 10 μM $Cygb^{3+}$ cannot be completely reduced even with the addition of as high as 30 mM Asc. Based on these observations, we proposed the following reaction mechanism for $Cygb^{3+}$ reduction by Asc:

$$Cygb^{3+} + A \underset{k_{-1}}{\overset{k_1}{\leftrightharpoons}} Cygb^{3+}A \underset{k_{-2}}{\overset{k_2}{\leftrightharpoons}} Cygb^{2+}A^{+} \quad (1)$$

Assuming that the initial $Cygb^{3+}$ concentration is c_0, the concentration of intermediate $Cygb^{3+}A$ is x, the concentration of product $Cygb^{2+}A^{+}$ is y, and the Asc concentration $[A]$ is a constant in each measurement because Asc concentration greatly exceeds c_0, we have the following equations when an equilibrium is reached:

$$k_1 (c_0 - x - y)[A] = k_{-1} x \quad (2)$$

$$k_2 x = k_{-2} y \quad (3)$$

From Eq. (3) we have:

$$y=\frac{k_2}{k_{-2}}x=K_2x \quad (4)$$

Substitution of Eq. (4) into (2) gives:

$$x=\frac{K_1c_0\,[A]}{1+K_1\,(1+K_2)\,[A]} \quad (5)$$

where $K_1=k_1/k_{-1}$. Substitution of Eq. (5) into (4) gives:

$$\frac{y}{c_0}=\frac{K_1K_2\,[A]}{1+K_1\,(1+K_2)\,[A]} \quad (6)$$

Eq. (6) indicates that the ratio of the equilibrium concentration of $Cygb^{2+}$ (y) to the initial $Cygb^{3+}$ concentration (c_0) increases with Asc concentration but will not approach 1 unless K_2 approaches infinity. We further experimentally examined the formation of $Cygb^{2+}$ in the presence of different Asc concentrations under anaerobic conditions at 37 °C by recording the change of absorbance at 428 nm with time on a Cary 50 spectrophotometer. From the $Cygb^{2+}$ equilibrium concentration (y) at each Asc concentration ([A]), we can plot the ratio y/c_0 (or $Cygb^{2+}/[Cygb^{3+}]_0$) vs. [A] (•) and then use Eq. (6) to fit the experimental data. As shown in Fig. 7, the best fitted curve (solid line) is in excellent agreement with the experimental data. From the best fitting curve, we obtained the value of K_1K_2 (0.0633±0.002 mM^{-1}) and the value of $K_1(1+K_2)$ (0.0751±0.0035 mM^{-1}) (n=7). The values of K_1 and K_2 calculated from the measured K_1K_2 and $K_1(1+K_2)$ are 0.012±0.006 mM^{-1} and 5.4±1.8, respectively.

Discussion

The rate of Mb-mediated NO consumption (Fig. 1A) is much less regulated by oxygen concentration than that of Cygb-mediated NO consumption (Fig. 1B). This large difference implies that the rate of $Cygb^{3+}$ reduction by Asc may be much greater than the rate of Mb^{3+} reduction by Asc. The rate of Mb^{3+} reduction by Asc is relatively slow (Fig. 2A) and the apparent first order rate constant is linear with Asc in the concentration range we examined (Fig. 2B). In contrast, the rate of Cygb reduction by Asc is much faster and the rate is not linear with Asc concentration[9]. Calculation from their rate constants gives that the reduction of $Cygb^{3+}$ by Asc is 415 times faster than the reduction of Mb by Asc. Using Eq. (8), the rate equation for Cygb[9], and the kinetic parameters in Table 1, we calculated $V_{Mb\text{-}NO}$-[O_2] and $V_{Cygb\text{-}NO}$-[O_2] curves, which fit the experimental data very well (Fig. 3). Our results show that in the presence of hundred μM Asc and sub μM globin, Mb-mediated NO consumption is much slower than the NO autoxidation rate making autoxidation the main component in the $V_{Mb\text{-}NO}$ term for the reaction with Mb. In contrast, Cygb-mediated NO consumption rather than NO autoxidation is the main component in the $V_{Cygb\text{-}NO}$ term. In Fig. 4, we demonstrate O_2 dependence of the Cygb and Mb mediated NO metabolism at three NO concentrations (10 nM, 1 nM and 0.1 nM) showing that the major working range of PO_2 for the Cygb-mediated NO metabolism in our experiments is within 0-31 torr (41 μM at 37 °C). The curve shifts to the left when [NO] decreases from 10 nM to 1 nM, but the

curve shift is very small when [NO] is further decreased from 1 nM to 0.1 nM. As a result of this shift, O_2 can more sharply regulate the Cygb-mediated NO consumption within the physiological range of NO concentration (low nM or below) when PO_2 is lower than 31 torr. It was reported that for wild type rats under normoxic conditions (21% O_2 in air), O_2 partial pressure (PO_2) is ~100 torr in the arteries, and 27 torr in tissues [33]. When the inspired O_2 tension dropped from 21% to 7% (hypoxia), PO_2 in tissues dropped below 10 torr. So PO_2 in these hypoxic tissues is within the major working range of PO_2 for the Cygb-mediated NO metabolism at physiological NO concentrations. Under the same conditions, the [O_2] working range for the Mb-mediated NO metabolism is only 0.32 torr, indicating that the rate of NO metabolism by Mb in the vascular wall does not change with [O_2] until [O_2] is below 0.32 torr. However, even if the Mb-mediated NO consumption can be regulated by O_2 concentration when [O_2] drops below 0.32 torr, this O_2 dependence of Mb-mediated NO metabolism is not important in the vascular wall because it is smaller than the rate of NO autoxidation (Fig. 3).

Computer simulations show that changes in oxygen concentration have little effect on concentrations of Mb^{3+}, $Mb^{2+}NO$, and $Mb^{2+}O_2$, under the experimental conditions of this study, and the majority of Mb exists in the form of Mb^{3+} due to the slow rate of Mb^{3+} reduction by Asc (Fig. 5). In contrast, concentrations of $Cygb^{3+}$, $Cygb^{2+}NO$, and $Cygb^{2+}O_2$ are very sensitive to changes in oxygen concentration. The high sensitivity of Cygb to transduce signals from changes in [O_2] into changes in the rate of NO consumption can be attributed to the significant formation rate of $Cygb^{2+}O_2$. Since the concentration increase of $Cygb^{2+}O_2$ is nearly 500 times greater than the concentration increase of $Mb^{2+}O_2$ in the oxygen concentration range between 0 and 50 μM, and the rate of NO dioxygenation by Cygb and Mb is proportional to $Cygb^{2+}O_2$ and $Mb^{2+}O_2$ concentration, respectively, this indicates that Cygb is nearly 500 times more sensitive than Mb for “detecting” changes of oxygen concentration in regulating the rate of NO consumption in the presence of ascorbate as reductant.

It is interesting that the reaction kinetics for the reduction of Cygb by Asc is very different from that of the reduction of Mb by Asc (Fig. 6). The existence of a corresponding equilibrium concentration of $Cygb^{2+}$ product for a given Asc concentration indicates that the reduction of $Cygb^{3+}$ by Asc is reversible. To explain the phenomenon that $Cygb^{3+}$ cannot be completely reduced by Asc even with Asc in gross excess, we suggest as reported previously[8] that Asc binds to $Cygb^{3+}$ prior to the reduction step. Thus, since the reduction is reversible, $Cygb^{3+}A$ cannot be completely converted into $Cygb^{2+}A^{+}$. Eq. (6) derived from the reaction mechanism shown in Eq. (1) fits the experimental data very well (Fig. 7), indicating that the proposed reaction mechanism can explain the experimental results for the reduction of $Cygb^{3+}$ by Asc. The physiological role of the reversible reduction of Cygb remains to be further understood; however, existence of this reversible reduction can prevent $Cygb^{3+}$ from being fully reduced to $Cygb^{2+}$ in hypoxia or anoxia. This lower concentration of reduced Cygb has a benefit in reducing the production of reactive oxygen species and decreasing the rate of NO consumption during reoxygenation.

If a globin acts as an oxygen sensor for the regulation of free NO and secondary vasodilation in the vascular wall, the rate of NO catabolism by this globin must be appropriate. If the NO

decay rate is too high in the vascular wall, the effective NO concentration may be too low to regulate vascular tone. Conversely, if the globin-mediated rate of NO catabolism is too low, this globin cannot be the major catabolic pathway to control NO concentration. Cygb seems to meet these requirements. Cygb concentration in tissue is nearly 4 orders of magnitude lower than Hb concentration in blood and nearly 2-3 orders of magnitude less than Mb concentration in skeletal and cardiac muscle. In this low concentration range, Cygb cannot act as an efficient NO scavenger as Hb and Mb do in RBCs[19, 21], skeletal and cardiac muscle[18, 20], but it is able to efficiently regulate the rate of NO metabolism in the vascular wall because $Cygb^{3+}$ can be rapidly recycled to $Cygb^{2+}$ by cellular reductants to continuously metabolize NO. Since the rate of Mb reduction by Asc is 2 orders of magnitude slower than Cygb, and the vascular wall contains only very low levels of Mb, vascular Mb cannot efficiently use cellular Asc as a reductant to metabolize NO. However, evidence has shown that Mb in myocardium can efficiently generate NO by reducing nitrite as O_2 concentration decreases [35]. This Mb-mediated NO generation from nitrite has protective effects on ischemia-reperfusion injury. It has been demonstrated that some other reductants and cellular reductases can efficiently supply electrons to $Cygb^{3+}$ for Cygb-mediated NO consumption, but these electron donors are not effective in supporting Mb-mediated NO consumption[8]. Cygb is a bis-histidyl hexacoordinate globin. It has been shown that bis-histidyl hexacoordination in globins facilitates heme reduction kinetics by small molecules[36]. These lines of evidence indicate that Cygb would be much more efficient than Mb in regulating NO metabolism in the vascular wall, where globin concentrations are in the range of low μM or less, by using cellular reductants as electron donors. In comparison, Mb is mainly present in skeletal or cardiac muscle where its high concentration enables O_2 storage, in turn facilitating O_2 diffusion in cardiac and skeletal muscles. The high concentration of Mb in these tissues along with its high affinity for O_2 enables a role in providing oxygen to the tissue under severe hypoxia. Its high rate of NO diooxygenation imparts its additional role in the oxidative degradation of NO in these muscles.

Materials and methods

Expression and Purification of recombinant Cygb

The expression plasmid for Cygb (human Cygb cDNA in pET3a) was obtained from Thorsten Burmester (Mainz, Germany) and transformed into *Escherichia coli* strain C41(DE3)pLysS. Cells were grown, harvested, and lysed as detailed in reference [9]. A 35 % ammonium sulfate cut was done on the supernatant, the pellet was discarded, and the supernatant was dialysed against 2 L of 50 mM TRIS-HCl, 1 mM dithiothreitol and 0.1 mM EDTA, pH 7.5 with a total of 3 buffer exchanges. After dialysis, insoluble material was removed by centrifugation (45,000 × g for 1 hour) and the human Cygb was concentrated to 50 mL using Amicon Ultra-15 centrifugal filters (Millipore Corporation) with a 10,000 molecular weight cutoff. Final purification was done on a GE Healthcare AKTA Purifier system using a 50 mL SuperLoop for sample loading. A HiPrep 16/10 DEAE FF anion-exchange column was run with a sodium chloride gradient elution followed by a HiPrep 26/60 Sephacryl S-300 High Resolution size-exclusion column eluted with 50 mM Tris-

HCl, pH 7.5, 100 mM NaCl, and 0.1 mM EDTA. The protein was concentrated and stored in 50 μL aliquots in a −80° C freezer.

Reduction of $Cygb^{3+}$ or Mb^{3+} by ascorbate

The reduction of $Cygb^{3+}$ and Mb^{3+} by Asc in a chamber (cuvette) was performed in a similar manner to that described in [9]. Briefly, the chamber was covered by Parafilm membrane and the buffer solution (pH 7.0, 37 °C) in the chamber was deaerated by bubbling argon gas into the solution for at least 15 minutes through a tube. After adding 10 μM deaerated $Cygb^{3+}$ or Mb^{3+} into the chamber, the tube was moved to the gas phase above the solution surface and the argon gas flow was maintained in the chamber during the experiments. After 5-10 minutes, varying concentrations of deaerated Asc were then added into the chamber using a Hamilton gastight syringe to start the reduction. The reduction of $Cygb^{3+}$ or Mb^{3+} in the solution was monitored using a Cary 50 UV/Vis spectrophotometer scanning from 350 nm to 700 nm or fixing the wavelength at the absorbance peak of the corresponding Soret band.

Simultaneous Measurements of [NO] and [O_2]

The measurements were performed in a 4-port water-jacketed electrochemical chamber (NOCHM-4 from WPI, Sarasota FL) containing 1 or 2 mL HyClone Dulbecco's Phosphate Buffered Saline (DPBS, pH 7.0, Thermo Scientific). A NO electrode and an O_2 electrode were connected to an Apollo 4000 electrochemical instrument (WPI, Sarasota FL). NO solution was prepared as described[5, 37]. To measure the rate of NO consumption by Cygb at different oxygen concentrations and to compare the results with that of Mb, NO (final concentration 0.5 μM) was added to the solution in the presence of 0.3 μM Cygb (or Mb), 300 μM Asc and 400 units/mL superoxide dismutase (SOD) to measure the rate of NO consumption in room air. Argon gas was then introduced in the chamber headspace to remove O_2 from the solution. While the oxygen concentration was gradually decreased by the flow of argon gas, 0.5 μM NO was repeatedly injected into the solution. From the recorded [*NO*]-*t* and [O_2]-*t* curves, the oxygen concentration and the NO decay rate (V_{NO}) at each NO peak were measured and used for plotting the V_{NO}-[O_2] curve.

Computer simulations of NO consumption by Cygb and Mb

Computer simulations of the rate of NO consumption by Cygb and Mb were performed on a PC using MATLAB software. The equations used in the simulations for Cygb are given in our previous paper[9]; and the equations for Mb are similar to those for Cygb except that the term k_h/k_{-h} is not involved:

$$V_{NO} = -\frac{k_1[E][NO][O_2]}{[O_2]\left(1+\frac{k_1[NO]}{k_2[R]}\right)+\left(\frac{k_{-3}}{k_3}+\frac{k_1}{k_3}[NO]\right)\left(1+\frac{k_4}{k_{-4}}[NO]\right)} \quad (7)$$

$$V_{Mb-NO} = V_{NO} + k_{au}[O_2][NO]^2 \quad (8)$$

$$\left[Mb^{2+}\right]=\frac{[E]}{1+\frac{k_4[NO]}{k_{-4}}+\left(1+\frac{k_1[NO]}{k_2[R]}\right)\frac{k_3[O_2]}{(k_{-3}+k_1[NO])}} \quad (9)$$

$$\left[Mb^{2+}O_2\right]=\frac{k_3\left[Mb^{2+}\right][O_2]}{k_{-3}+k_1[NO]} \quad (10)$$

$$\left[Mb^{3+}\right]=\frac{k_1k_3\left[Mb^{2+}\right][O_2][NO]}{k_2[R](k_{-3}+k_1[NO])} \quad (11)$$

$$\left[Mb^{2+}NO\right)\left]=\frac{k_4\left[Mb^{2+}\right][NO]}{k_{-4}} \quad (12)$$

In the above equations, V_{NO} is the rate of NO consumption by Mb, [E] is the total Mb concentration, [R] is the Asc concentration, $V_{Mb\text{-}NO}$ is the sum of V_{NO} and the rate of NO autoxidation in solution as defined in Eq. (8).

Conclusion

The rate of metCygb reduction by Asc is hundreds of times greater than the rate of metMb reduction by Asc. As a result, Cygb regulates the rate of NO catabolism in response to a change in oxygen concentration nearly 500 times more efficiently than its family member Mb. In addition to the large difference in the rate constants between Cygb reduction and Mb reduction by Asc, the reduction of Cygb by Asc is reversible so that $Cygb^{3+}$ cannot be fully reduced to $Cygb^{2+}$ in the presence of mM or even tens of mM Asc. The rapid reduction of Cygb by cellular reductants enables Cygb to efficiently regulate the oxygen-dependent NO metabolism in the vascular wall.

Acknowledgments

This work was supported by National Institutes of Health grants HL063744, HL065608, and HL38324. We also thank undergraduate students Kaitlyn Boggs, Caty P. Escobar, Rachael Huskey, Yeram Kang, and Mariel McGuiness for their volunteer work in our lab.

Abbreviations

Cygb	cytoglobin
Mb	myoglobin
Ngb	neuroglobin
$Hb^{2+}O_2$	oxyhemoglobin
$Mb^{2+}O_2$	oxymyoglobin
$Ngb^{2+}O_2$	oxyneuroglobin

$Cygb^{2+}O_2$	oxycytoglobin
Asc	ascorbate
NO	nitric oxide
O_2	oxygen
PO_2	O_2 partial pressure

References

1. Halligan KE, Jourd'heuil FL, Jourd'heuil D. Cytoglobin is expressed in the vasculature and regulates cell respiration and proliferation via nitric oxide dioxygenation. J Biol Chem. 2009; 284:8539–47. [PubMed: 19147491]
2. Straub AC, Lohman AW, Billaud M, Johnstone SR, Dwyer ST, Lee MY, Bortz PS, Best AK, Columbus L, Gaston B, Isakson BE. Endothelial cell expression of haemoglobin alpha regulates nitric oxide signalling. Nature. 2012; 491:473–7. [PubMed: 23123858]
3. Kelm M, Schrader J. Control of coronary vascular tone by nitric oxide. Circ Res. 1990; 66:1561–75. [PubMed: 2160870]
4. Moncada S, Radomski MW, Palmer RM. Endothelium-derived relaxing factor. Identification as nitric oxide and role in the control of vascular tone and platelet function. Biochem Pharmacol. 1988; 37:2495–501. [PubMed: 3291879]
5. Thomas DD, Liu X, Kantrow SP, Lancaster JR Jr. The biological lifetime of nitric oxide: implications for the perivascular dynamics of NO and O2. Proc Natl Acad Sci U S A. 2001; 98:355–60. [PubMed: 11134509]
6. Liu X, Srinivasan P, Collard E, Grajdeanu P, Lok K, Boyle SE, Friedman A, Zweier JL. Oxygen regulates the effective diffusion distance of nitric oxide in the aortic wall. Free Radic Biol Med. 2010; 48:554–9. [PubMed: 19969071]
7. Smagghe BJ, Trent JT 3rd, Hargrove MS. NO dioxygenase activity in hemoglobins is ubiquitous in vitro, but limited by reduction in vivo. PLoS One. 2008; 3:e2039. [PubMed: 18446211]
8. Gardner AM, Cook MR, Gardner PR. Nitric-oxide dioxygenase function of human cytoglobin with cellular reductants and in rat hepatocytes. J Biol Chem. 2010; 285:23850–7. [PubMed: 20511233]
9. Liu X, Follmer D, Zweier JR, Huang X, Hemann C, Liu K, Druhan LJ, Zweier JL. Characterization of the function of cytoglobin as an oxygen-dependent regulator of nitric oxide concentration. Biochemistry. 2012; 51:5072–82. [PubMed: 22577939]
10. Eich RF, Li T, Lemon DD, Doherty DH, Curry SR, Aitken JF, Mathews AJ, Johnson KA, Smith RD, Phillips GN Jr. Olson JS. Mechanism of NO-induced oxidation of myoglobin and hemoglobin. Biochemistry. 1996; 35:6976–83. [PubMed: 8679521]
11. Herold S, Exner M, Nauser T. Kinetic and mechanistic studies of the NO*-mediated oxidation of oxymyoglobin and oxyhemoglobin. Biochemistry. 2001; 40:3385–95. [PubMed: 11258960]
12. Hardison RC. A brief history of hemoglobins: plant, animal, protist, and bacteria. Proc Natl Acad Sci U S A. 1996; 93:5675–9. [PubMed: 8650150]
13. Garry DJ, Kanatous SB, Mammen PP. Emerging roles for myoglobin in the heart. Trends Cardiovasc Med. 2003; 13:111–6. [PubMed: 12691675]
14. Burmester T, Weich B, Reinhardt S, Hankeln T. A vertebrate globin expressed in the brain. Nature. 2000; 407:520–3. [PubMed: 11029004]
15. Pesce A, Bolognesi M, Bocedi A, Ascenzi P, Dewilde S, Moens L, Hankeln T, Burmester T. Neuroglobin and cytoglobin. Fresh blood for the vertebrate globin family. EMBO Rep. 2002; 3:1146–51. [PubMed: 12475928]
16. Hankeln T, Ebner B, Fuchs C, Gerlach F, Haberkamp M, Laufs TL, Roesner A, Schmidt M, Weich B, Wystub S, Saaler-Reinhardt S, Reuss S, Bolognesi M, De Sanctis D, Marden MC, Kiger L, Moens L, Dewilde S, Nevo E, Avivi A, Weber RE, Fago A, Burmester T. Neuroglobin and

cytoglobin in search of their role in the vertebrate globin family. J Inorg Biochem. 2005; 99:110–9. [PubMed: 15598495]

17. Liu X, Miller MJ, Joshi MS, Sadowska-Krowicka H, Clark DA, Lancaster JR Jr. Diffusion-limited reaction of free nitric oxide with erythrocytes. J Biol Chem. 1998; 273:18709–13. [PubMed: 9668042]
18. Flogel U, Merx MW, Godecke A, Decking UK, Schrader J. Myoglobin: A scavenger of bioactive NO. Proc Natl Acad Sci U S A. 2001; 98:735–40. [PubMed: 11136228]
19. Jeffers A, Xu X, Huang KT, Cho M, Hogg N, Patel RP, Kim-Shapiro DB. Hemoglobin mediated nitrite activation of soluble guanylyl cyclase. Comp Biochem Physiol A Mol Integr Physiol. 2005; 142:130–5. [PubMed: 15936233]
20. Merx MW, Godecke A, Flogel U, Schrader J. Oxygen supply and nitric oxide scavenging by myoglobin contribute to exercise endurance and cardiac function. Faseb J. 2005; 19:1015–7. [PubMed: 15817640]
21. Liu X, Yan Q, Baskerville KL, Zweier JL. Estimation of nitric oxide concentration in blood for different rates of generation. Evidence that intravascular nitric oxide levels are too low to exert physiological effects. J Biol Chem. 2007; 282:8831–6. [PubMed: 17267398]
22. Lechauve C, Chauvierre C, Dewilde S, Moens L, Green BN, Marden MC, Celier C, Kiger L. Cytoglobin conformations and disulfide bond formation. Febs J. 2010; 277:2696–704. [PubMed: 20553503]
23. Fago A, Hundahl C, Malte H, Weber RE. Functional properties of neuroglobin and cytoglobin. Insights into the ancestral physiological roles of globins. IUBMB Life. 2004; 56:689–96. [PubMed: 15804833]
24. Burmester T, Ebner B, Weich B, Hankeln T. Cytoglobin: a novel globin type ubiquitously expressed in vertebrate tissues. Mol Biol Evol. 2002; 19:416–21. [PubMed: 11919282]
25. Lawrie, RA. Lawrie's meat science. sixth edn. Woodhead Publishing; Cambridge: 1998.
26. Tsukahara K, Okazawa T, Takahashi H, Yamamoto Y. Kinetics of Reduction of Metmyoglobins by Ascorbate. Effect of the Modification of the Heme Distal Side, Heme Propionates, and 2,QSubstituents of Deuterohemin. Inorg Chem. 1986; 25:4756–4760.
27. Doyle MP, Pickering RA, Cook BR. Oxidation of oxymyoglobin by nitric oxide through dissociation from cobalt nitrosyls. Journal of Inorganic Biochemistry. 1983; 19:329–338.
28. Doyle MP, Hoekstra JW. Oxidation of nitrogen oxides by bound dioxygen in hemoproteins. J Inorg Biochem. 1981; 14:351–8. [PubMed: 7276933]
29. Schenkman KA, Marble DR, Burns DH, Feigl EO. Myoglobin oxygen dissociation by multiwavelength spectroscopy. J Appl Physiol. 1997; 82:86–92. [PubMed: 9029202]
30. Hall CN, Garthwaite J. What is the real physiological NO concentration in vivo? Nitric Oxide. 2009; 21:92–103. [PubMed: 19602444]
31. Wood KC, Batchelor AM, Bartus K, Harris KL, Garthwaite G, Vernon J, Garthwaite J. Picomolar nitric oxide signals from central neurons recorded using ultrasensitive detector cells. J Biol Chem. 2011; 286:43172–81. [PubMed: 22016390]
32. May JM, Qu ZC, Qiao H. Transfer of ascorbic acid across the vascular endothelium: mechanism and self-regulation. Am J Physiol Cell Physiol. 2009; 297:C169–78. [PubMed: 19419995]
33. Johnson PC, Vandegriff K, Tsai AG, Intaglietta M. Effect of acute hypoxia on microcirculatory and tissue oxygen levels in rat cremaster muscle. J Appl Physiol. 2005; 98:1177–84. [PubMed: 15772057]
34. Guazzi M, Freis ED. Sino-aortic reflexes and arterial pH, PO2, and PCO2 in wakefulness and sleep. Am J Physiol. 1969; 217:1623–7. [PubMed: 4311015]
35. Hendgen-Cotta UB, Merx MW, Shiva S, Schmitz J, Becher S, Klare JP, Steinhoff HJ, Goedecke A, Schrader J, Gladwin MT, Kelm M, Rassaf T. Nitrite reductase activity of myoglobin regulates respiration and cellular viability in myocardial ischemia-reperfusion injury. Proc Natl Acad Sci U S A. 2008; 105:10256–61. [PubMed: 18632562]
36. Weiland TR, Kundu S, Trent JT 3rd, Hoy JA, Hargrove MS. Bis-histidyl hexacoordination in hemoglobins facilitates heme reduction kinetics. J Am Chem Soc. 2004; 126:11930–5. [PubMed: 15382928]

37. Liu X, El-Sherbiny GA, Collard E, Huang X, Follmer D, El-Mahdy M, Zweier JL. Application of carbon fiber composite minielectrodes for measurement of kinetic constants of nitric oxide decay in solution. Nitric Oxide. 2010; 23:311–8. [PubMed: 20854922]

38. Hamdane D, Kiger L, Dewilde S, Green BN, Pesce A, Uzan J, Burmester T, Hankeln T, Bolognesi M, Moens L, Marden MC. The redox state of the cell regulates the ligand binding affinity of human neuroglobin and cytoglobin. J Biol Chem. 2003; 278:51713–21. [PubMed: 14530264]

39. Cutruzzola F, Travaglini Allocatelli C, Brancaccio A, Brunori M. Aplysia limacina myoglobin cDNA cloning: an alternative mechanism of oxygen stabilization as studied by active-site mutagenesis. Biochem J. 1996; 314(Pt 1):83–90. [PubMed: 8660313]

40. Gibson QH, Olson JS, McKinnie RE, Rohlfs RJ. A kinetic description of ligand binding to sperm whale myoglobin. J Biol Chem. 1986; 261:10228–39. [PubMed: 3733708]

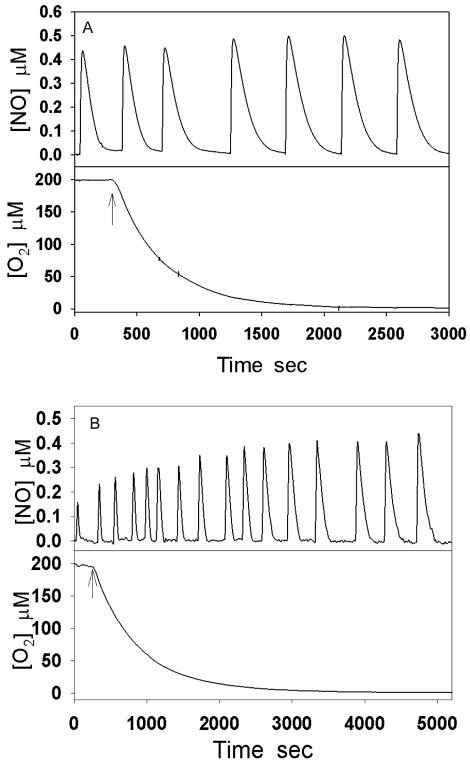

Fig. 1.

Measurements of oxygen-dependent NO consumption rate. NO (final concentration 0.5 μM) was repeatedly added to the solution in the presence of 0.3 μM Mb (A) or Cygb (B), 300 μM Asc and 400 units/mL SOD. The upwards arrows designate the time that argon gas started to flow over the solution surface to remove oxygen in the solution.

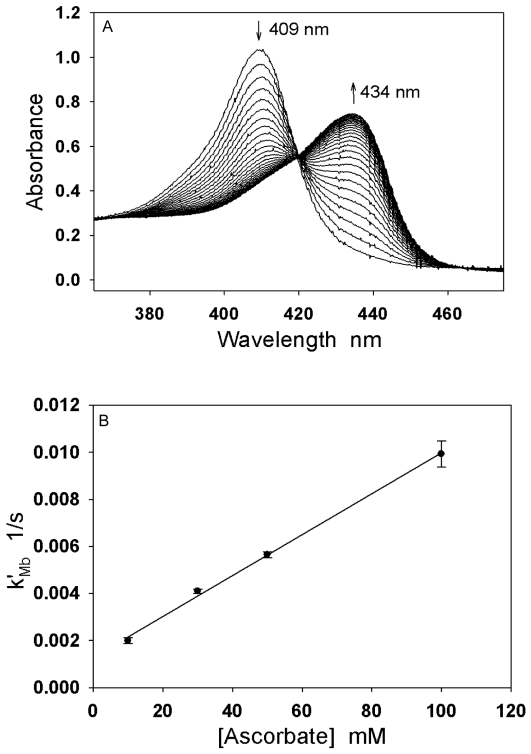

Fig. 2.

Reduction of Mb by Asc. (A) An illustration of reduction of 10 μM Mb(Fe^{3+}) to Mb(Fe^{2+}) by 10 mM ascorbate at 37 °C under anaerobic conditions, which was indicated by a shift of the heme Soret band from 409 nm to 434 nm. (B) The second order rate constant k_{Mb} at 37 °C was determined as (8.7 ± 0.3) × 10^{-2} $M^{-1}s^{-1}$ (n=5) by the plot of the pseudo first order rate constant k'_{Mb} versus Asc concentration (10-100 mM).

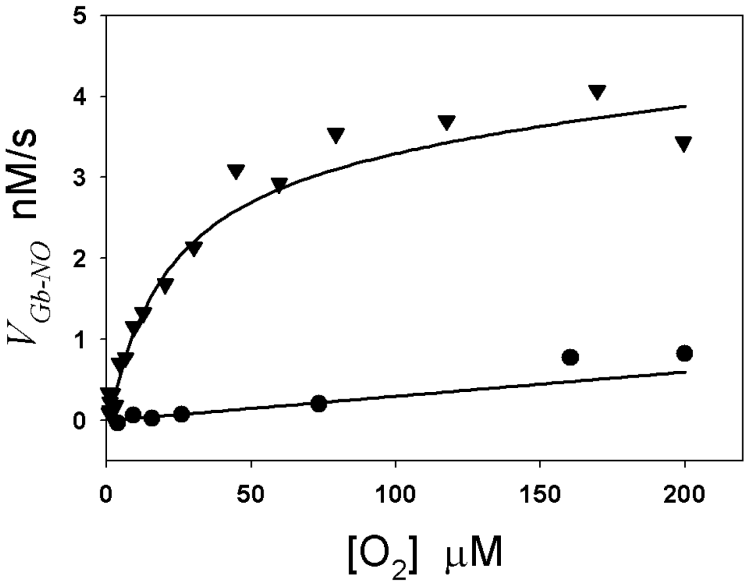

Fig. 3.

Simulated and measured $V_{Cygb\text{-}NO}$-[O_2] and $V_{Mb\text{-}NO}$-[O_2] curves at varying O_2 concentrations. Experimental data $V_{Mb\text{-}NO}$ (•) and $V_{Cygb\text{-}NO}$ (▽) versus [O_2] were obtained from Figs. 1A and 1B, respectively. The $V_{Mb\text{-}NO}$-[O_2] and $V_{Cygb\text{-}NO}$-[O_2] curves (solid lines) were simulated from Eqs. (7)&(8) and equations in our previous paper[9]. In the simulations, [NO] is 500 nM, Asc concentration is 0.3 mM, and all other parameters are listed in Table 1.

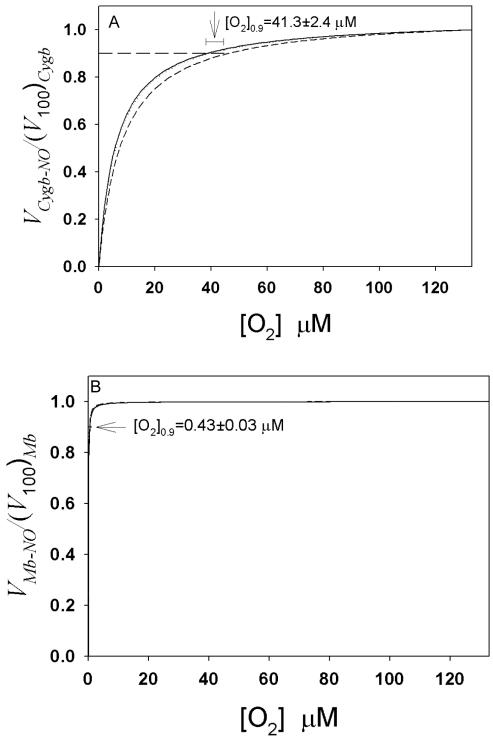

Fig. 4.

Computer simulations to examine the O_2 dependence of Cygb- and Mb-mediated NO consumption at different NO concentrations. The normalized rate of Cygb-mediated NO metabolism (A) and Mb-mediated NO metabolism (B) versus $[O_2]$ were simulated at [NO]=10 nM (dashed), 1 nM (dotted) and 0.1 nM (solid) (In A, the [NO] = 1 nM and [NO] = 0.1 nM curves are nearly overlapping, while in B, all curves nearly overlap), and [Asc]=1 mM [32]. Other related parameters for computer simulations are listed in Table 1. $(V_{100})_{Cygb}$ and $(V_{100})_{Mb}$ are the rates of NO metabolism by Cygb and Mb at PO_2=100 torr, respectively. $[O_2]$ working range for regulating the Cygb-mediated NO metabolism is from 0 to $[O_2]$ corresponding to the normalized rate at 0.9, which is 41.3±2.4 μM for Cygb and 0.43±0.03 μM for Mb.

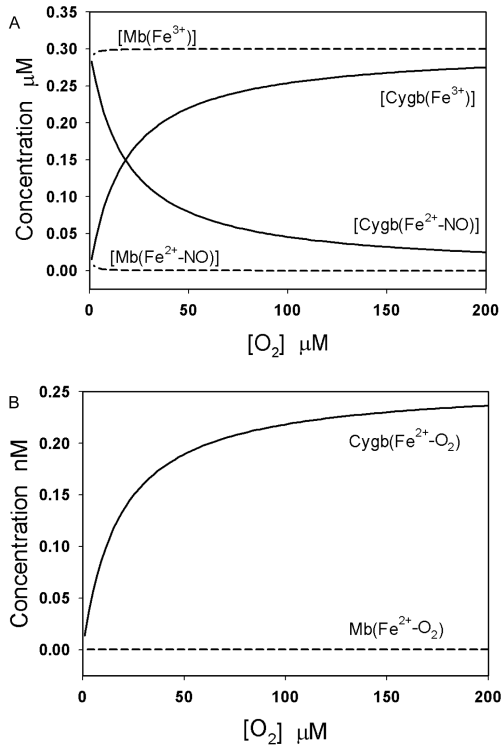

Fig. 5.

Effect of oxygen concentration on globin species. A: Simulated concentration changes of Cygb(Fe^{3+}), Cygb(Fe^{2+}NO), Mb(Fe^{3+}) and Mb(Fe^{2+}NO) when [O_2] varies from 0 to 200 μM. B: Simulated concentration changes of Cygb($Fe^{2+}O_2$) and Mb($Fe^{2+}O_2$) when [O_2] varies from 0 to 200 μM.

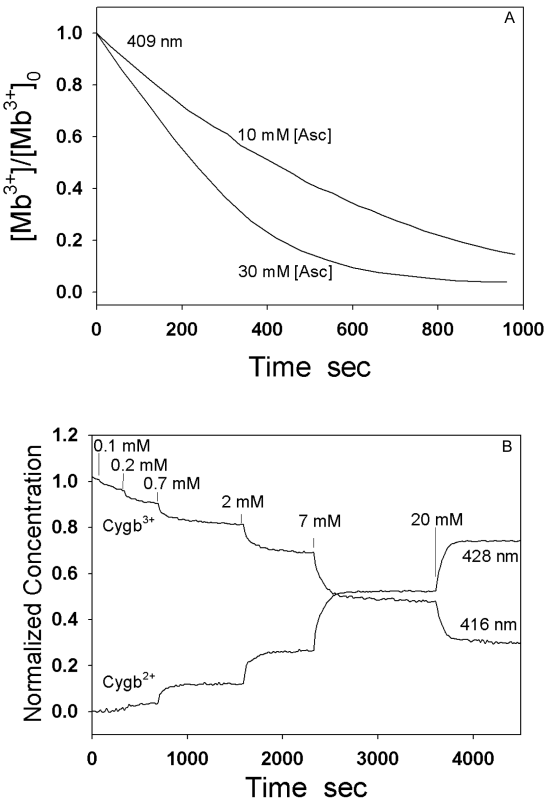

Fig. 6.

Kinetic characteristics of reduction of Mb^{3+} and $Cygb^{3+}$ by different concentrations of Asc. A: Reduction of Mb^{3+} by 10 mM and 30 mM Asc. B: Simultaneous measurements of $Cygb^{3+}$ reduction and $Cygb^{2+}$ formation at different Asc concentrations. The reaction process of $Cygb^{3+}$ with Asc was recorded by repetitively scanning from 350 nm and 700 nm on a Cary 50 UV/VIS spectrophotometer while different concentrations of Asc (0.1, 0.2, 0.7, 2, 7, 20 mM) were injected into the chamber at the time indicated by vertical lines. The kinetic curves of $Cygb^{3+}$ reduction and $Cygb^{2+}$ formation can be observed by plotting the absorbance changes vs. time at wavelength 416 nm or 428 nm.

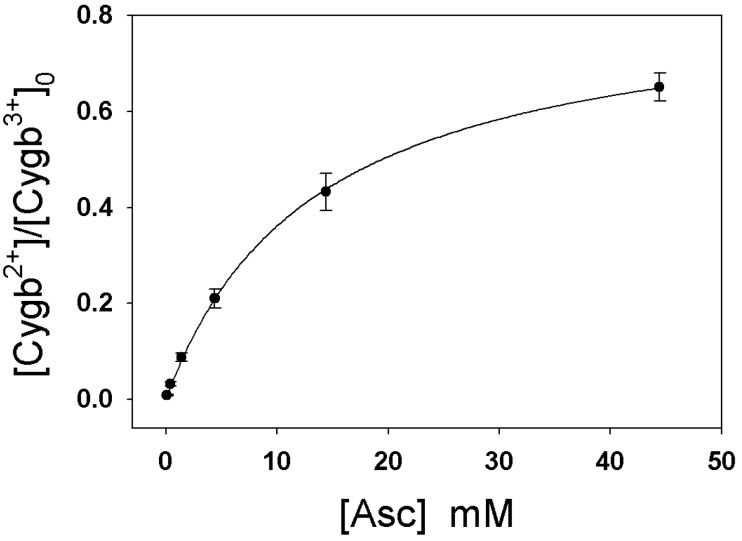

Fig. 7.

Plot of $Cygb^{2+}/[Cygb^{3+}]_0$ vs. [*A*]. Eq. (6) is used to fit the experimental data (•). The best fitted curve (solid line) is in excellent agreement with the experimental data (n=7). The values of K_1K_2 (0.0633 ± 0.002 mM^{-1}) and $K_1(1+K_2)$ (0.0751 ± 0.0035 mM^{-1}) were obtained from the best fitting curve. The values of K_1 and K_2 calculated from the measured K_1K_2 and $K_1(1+K_2)$ are 0.012 ± 0.006 mM^{-1} and 5.4 ± 1.8, respectively.

Table 1

Kinetic and equilibrium constants involved in the oxygen-dependent NO consumption by Cygb and Mb.

Parameters	Values for Cygb	References	Values for Mb	References
k_1	2.2×10^7 $M^{-1}s^{-1}$ (20 °C) **3×10^7 $M^{-1}s^{-1}$ (37 °C)**	[7] [9]	3.1×10^7 $M^{-1}s^{-1}$ (10 °C) 3.4×10^7 $M^{-1}s^{-1}$ (20 °C) 3.7×10^7 $M^{-1}s^{-1}$ (25 °C) **4.5×10^7 $M^{-1}s^{-1}$ (37 °C)**	[27] [10] [28] Estimated
k_2 (k_{Cygb} or k_{Mb})	36 **(56) M^{-1} s^{-1} (37 °C)**	[9]	**8.7×10^{-2} $M^{-1}s^{-1}$ (37 °C)**	This work
k_{-3}/k_3	35 nM (25 °C) **37 nM (37 °C)**	[22] [9]	**3.2 μM (2.4 torr) (37 °C)**	[29]
k_{-3}	0.9 s^{-1} (25 °C) **1.3 s^{-1} (37 °C)**	[38] [9]	**15 s^{-1} (37 °C)**	[39]
k_3	2.5×10^7 $M^{-1}s^{-1}$ (25 °C) 2.7×10^7 $M^{-1}s^{-1}$ (25 °C) **3.5×107 $M^{-1}s^{-1}$ (37 °C)**	[22] [38] [9]	**1.7×10^7 $M^{-1}s^{-1}$ (37 °C)**	[39]
k_h/k_{-h}	140(25 °C) **165 (37 °C)**	[22] [9]		
k_4			1.7×10^7 $M^{-1}s^{-1}$ (20 °C)	[40]
k_{-4}			1.2×10^{-4} s^{-1} (20 °C)	[40]
k_{-4}/k_4	**8 pM (37 °C)**	[9]	**35 pM (37 °C)**	Estimated
k_{au}	**11×10^6 $M^{-2}s^{-1}$ (37 °C)**	[37]	**11×10^6 $M^{-2}s^{-1}$ (37 °C)**	